

Proposed Modification to the WFPC2 SAA Avoidance Contour

J. Biretta and S. Baggett
June 19, 2009

ABSTRACT

We have examined cosmic ray rates taken inside and around the South Atlantic Anomaly (SAA). Based on those results, we propose a new, slightly smaller WFPC2 SAA avoidance region. The new SAA contour should help improve HST scheduling efficiency with minimum impact to WFPC2 observations.

1. Introduction

The South Atlantic Anomaly (SAA) is a region where irregularities in the Earth's magnetic field cause very high cosmic ray rates. WFPC2 imaging is generally not scheduled near the SAA, so as to avoid excessive cosmic ray hits which degrade images by obliterating data in numerous pixels. The same is true for STIS CCD observations. Other instruments, such as the STIS MAMAs, are not scheduled near the SAA because particle impacts can upset the instrument control electronics, thus disrupting observations or even possibly damaging the instrument if its controls were affected at an inopportune time. These adverse effects are usually minimized by operating each instrument only when HST is outside a designated "SAA avoidance contour." Each instrument has its own contour based upon its cosmic ray tolerance.

Avoiding the SAA obviously affects HST scheduling. In the simplest sense, the geometric area of the SAA reduces the amount of HST time available for scheduling observations by several hundred orbits per year. In practice, however, the impact is even larger. Since HST time is granted in units of "orbits," observers make every effort to construct visits which completely fill the allocated orbits. As a consequence, most visits will not fit into orbits which intersect the SAA, even if the intersection lasts a brief few minutes. The schedulers attempt to minimize the impact by selecting targets where the Earth occultation hides the SAA, but this approach is only partly effective. In addition, some observations, such as STIS MAMA observations, require long periods of continuous

SAA-free orbits. Currently, the limit is ~ 7 contiguous SAA-free orbits using the STIS SAA avoidance contour (Baum et al., 1998), while the larger WFPC2 contour allows only ~ 6 contiguous orbits. Hence the WFPC2 SAA contour limits opportunities for scheduling STIS observations in parallel with WFPC2. For these reasons, there is considerable interest in reducing the size of the SAA contours wherever possible.

In this report, we examine cosmic ray rates inside and around the SAA, and recommend a slightly smaller SAA avoidance region for WFPC2. The new contour should improve HST scheduling efficiency while posing minimal risk to WFPC2 observations.

2. WFPC2 Cosmic Ray Rates Inside and Outside the SAA

In this section we examine the WFPC2 cosmic ray rates at different points of the HST orbit inside, near, and outside the SAA.

For purposes of studying relative cosmic ray rates, we measure the rates as the number of pixels in an image exceeding 20 DN per CCD per second. We use this metric since it is easily applied to images with *wstat* in IRAF. A single cosmic ray “hit” corrupts any number of pixels from a few to perhaps hundreds for cosmic rays which strike the CCD at a grazing angle. So, merely counting pixels does not provide the number of “hits,” but it does yield a useful relative number, and more specifically, tells us what we need to know - that is, the number of pixels which become corrupted. The choice of threshold at 20 DN omits outlying pixels which are weakly affected by cosmic ray “hits,” but again, we are primarily interested in relative cosmic ray rates. This threshold has the advantage that it will be largely immune to fluctuations in background levels. (For example, some of the planetary images used have significant backgrounds from scattered light.)

We have identified several hundred WFPC2 images taken inside and near the SAA. These are primarily short exposures of planetary events, where timing constraints have forced the observation inside the SAA. In many cases, planetary targets were present on the CCD frames, but we avoided using those regions of the CCD. In computing the cosmic ray rate, we have used the effective “exposure time” for cosmic rays, taking into account the WFPC2 overhead times and commanding sequences, rather than simply using the exposure time from the image header. Wherever possible, measurements were made separately for each CCD.

We begin by examining the distribution of cosmic ray rates, in an effort to characterize “nominal” rates and rates inside and near the SAA. Figure 1 presents histograms of the cosmic ray rates for external images taken inside and near the SAA, as well as for a series of dark calibration exposures. The data within the current WFPC2 M25 SAA contour (Figure 1a) show a Gaussian distribution centered around 12 pixels/sec/CCD with the distribution width corresponding roughly to $\sigma=5$ pixels/sec/CCD. The distribution also has a significant tail extended to ~ 100 pixels/sec/CCD.

Similarly, Figure 1b shows the distribution for data taken outside (primarily near) the SAA. Again, there is a Gaussian distribution at low rates, centered at about 8 pixels/sec/CCD, with a sigma of about 3 pixels/sec/CCD. There is also a tail extending to high rates, but there are very few events within the tail as compared to Figure 1a.

We have also examined cosmic ray rates for long exposures taken away from the SAA. Specifically, we examined 120 dark calibration exposures taken in 1997 and 1998, each 1800 sec in duration. Figure 1c shows a histogram of the measured cosmic ray rates for the PC CCD dark images. The mean rate is 6.5 pixels/sec/CCD. The spread of the distribution is relatively narrow: the standard deviation is 1.4 pixels/sec/CCD or 21% of the mean, and the range is 5 to 11. We will take these results for long dark images as representative of the rates seen for long WFPC2 science exposures (typical exposures 600s - 1500s) using the current avoidance contours.

Note that the distribution for the dark frames (Figure 1c) is much narrower than that of the shorter exposures (Figure 1b). This is partly due to many of the images in Figure 1b being located near the SAA (see also Figures 2 and 3). An additional factor is the length of the exposures: any variations in cosmic ray rates over a short timescale will be averaged out in the longer dark exposures (1800 s) while rates in short (~60 s) exposures will experience very little averaging.

Figure 1: Histograms of cosmic ray rates inside and outside the SAA. (a) Data from Figure 2 within SAA contour M25. (b) Data from Figure 2 outside SAA contour M25. (c) Data for 120 dark frames. Figures in (d-f) are the same as (a-c) but with a logarithmic horizontal axis.

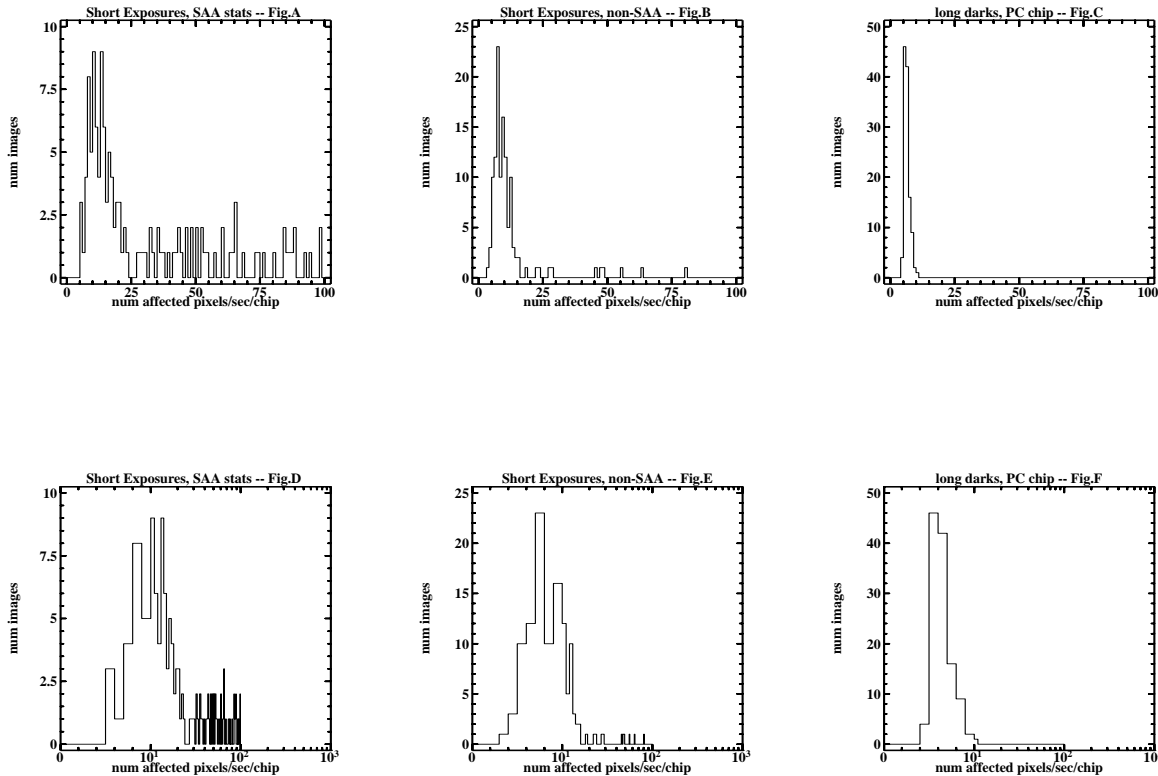
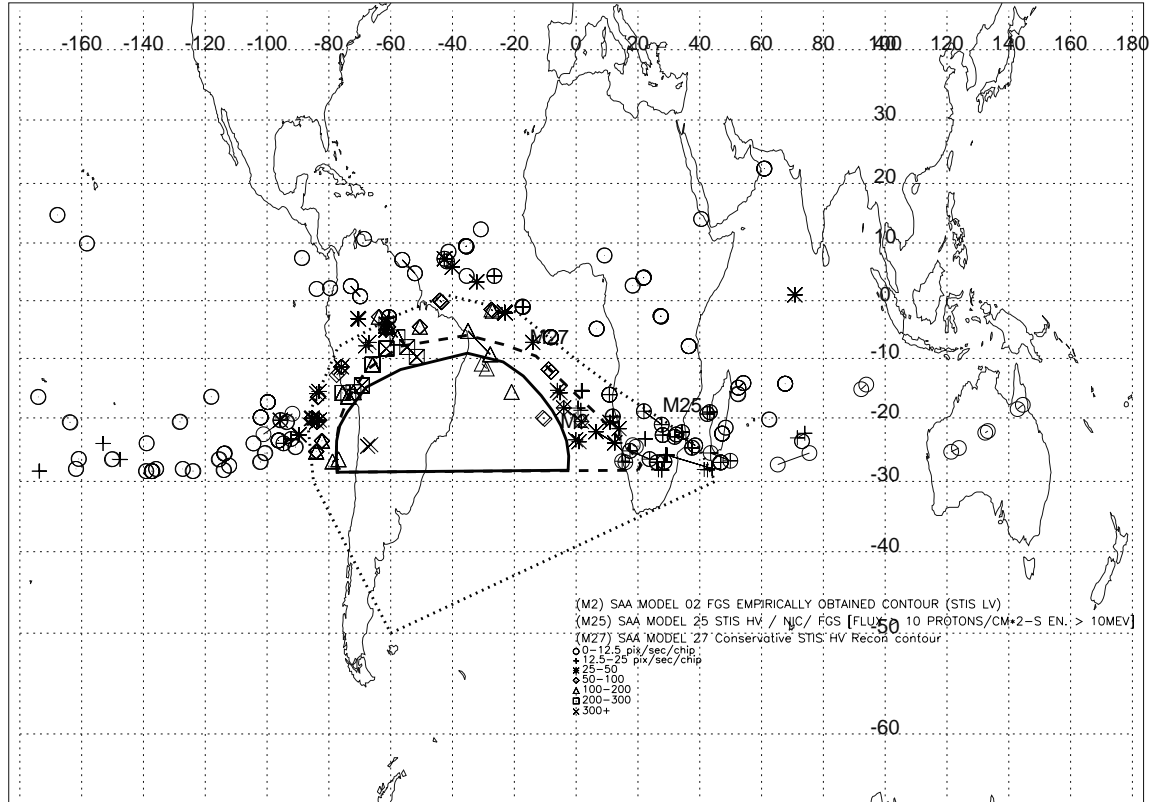


Figure 2 presents the measured rates as a function of HST position around the Earth for the short exposures described above; Figure 3 shows an enlargement of the region near the SAA. The different symbols represent various cosmic ray rates as noted in the plot's legend. In many instances, there are several symbols superposed; these occur when different CCDs gave slightly different rates for the same exposure. There are also cases where two symbols are joined by a line segment; these are exposures typically 2-3 minutes long; the two joined points mark the HST position at the start and end of the exposure. These figures also illustrate the current WFPC2 SAA avoidance contour (M25, dotted line), the STIS contour (M27, dashed line), and the FGS guiding contour (M2, solid line).

Figure 2: Cosmic ray rates in WFPC2 images as a function of HST position projected onto the Earth. Plotting software and SAA contours were provided by B.Sawchuck.



Figures 2 and 3 reveal several interesting features:

(1) The current WFPC2 contour seems quite sensible -- rates are generally low outside the contour (<12.5 pixels/sec/CCD, or less than twice the mean value for long darks).

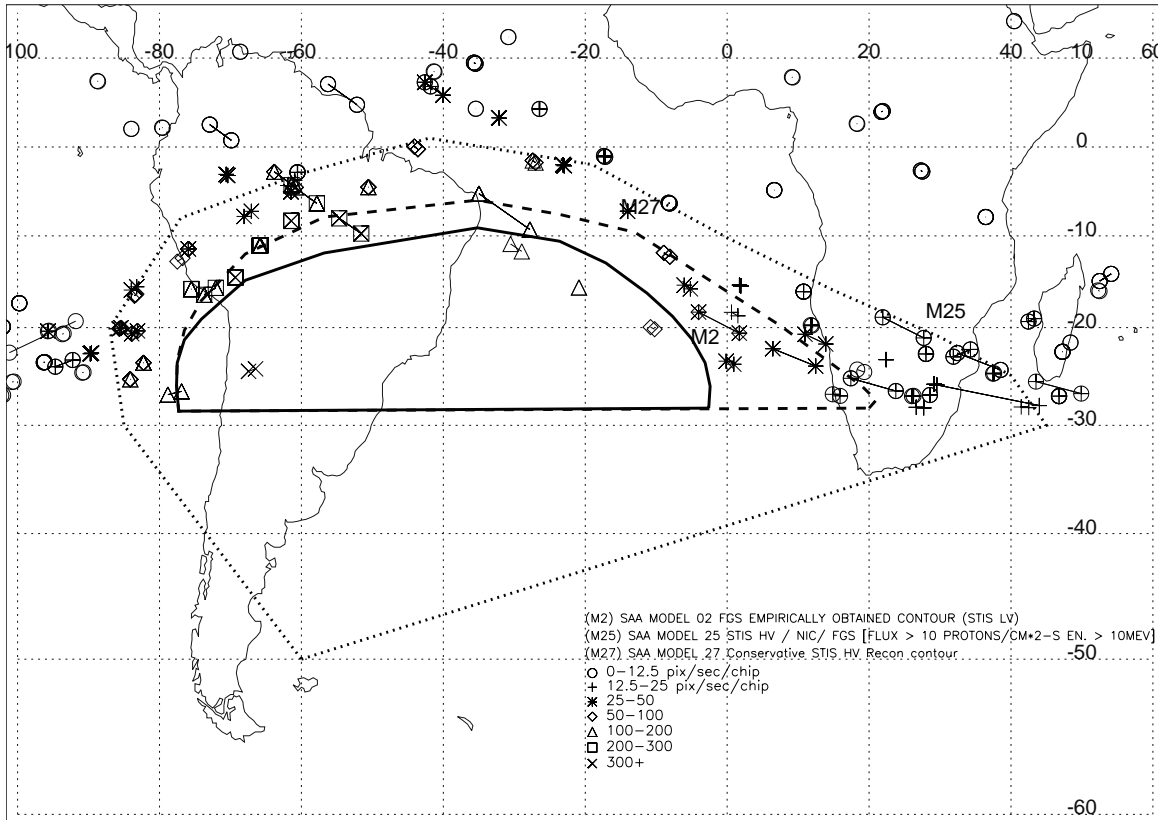
(2) The SAA causes a large perturbation in the cosmic ray rates. The highest rates inside the SAA are more than fifty times the mean rate outside the SAA for the long dark exposures.

(3) On the eastern side of the SAA, just inside the current WFPC2 contour (M25), the rates remain relatively low (<25 pixels/sec/CCD, or less than four times the mean rate in the 1800 sec dark frames). Reduction of the avoidance contour in this region should present relatively low risk to WFPC2 observations.

(4) On the western side of the SAA, the rates rise rapidly just inside the M25 contour. Values in the 50-100 pixels/sec/CCD range (about ten times the mean rate for the darks) are fairly common just inside the M25 contour.

(5) There are also small regions outside the M25 contour where elevated rates are seen (e.g. 25 - 50 pixels/sec/CCD, seen north of the SAA, near latitude +10, longitude -40).

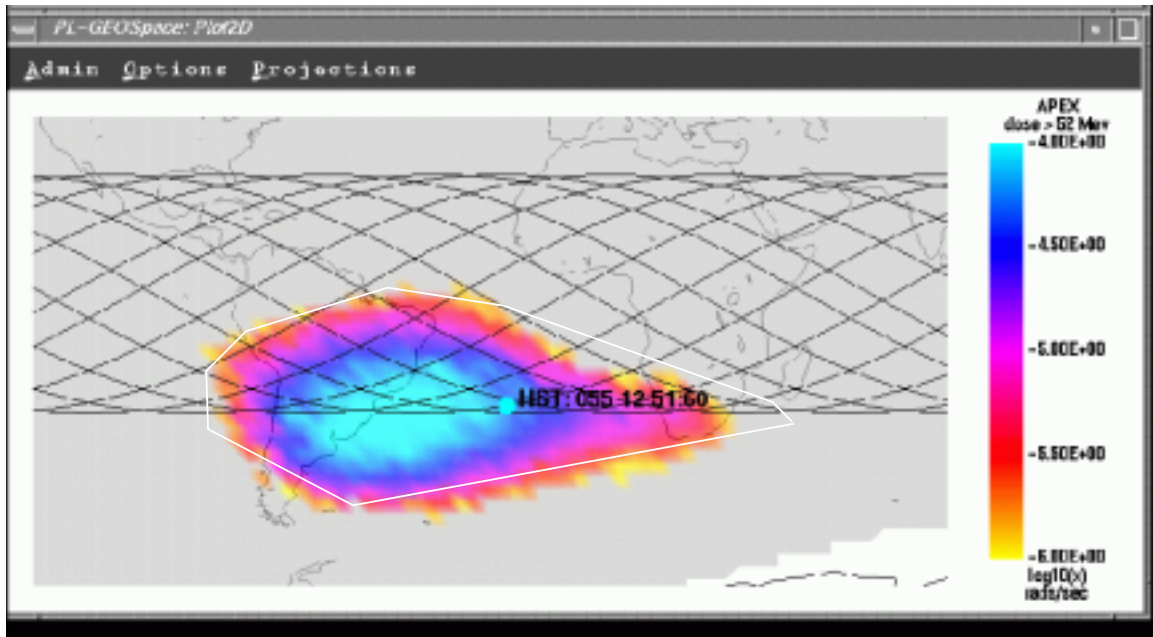
Figure 3: Same as Figure 1, but with SAA region enlarged.



3. Air Force Satellite Data

An additional source of cosmic ray rate information are data taken by USAF satellites. These results originate from Philips Laboratory at Hanscom AFB, and were provided locally by Bill Sawchuck. The data were taken by an APEX satellite at 600-625 km altitude. Figure 4 shows the flux in rads / sec of particles with energies >52 Mev. The approximate outline of the M25 contour has been superposed. The data seem to confirm the results seen in Figure 3: the cosmic ray rates just inside the eastern portion of the M25 contour are relatively low, while on the western side of the SAA, the rate rises rapidly just inside the M25 contour.

Figure 4: USAF data from the APEX satellite with HST M25 SAA avoidance contour superposed.



4. STIS CCD Data

A third source of information are special STIS CCD observations taken during a single pass of HST through the SAA on 01 Mar 1997. The images consist of a sequence of 60s dark exposures taken specifically to map cosmic ray rates inside the SAA. Detailed descriptions are given in Lindler (1997), with summaries reported by Baum, Reinhart, and Ferguson (1998). Figure 5 shows the position of HST during each of the 19 STIS images along with the SAA contours M2 (FGS), M25 (WFPC2), and M27 (STIS); Figure 6 presents the cosmic ray rate at each point.

Figure 5: Locations of HST for STIS CCD 60s darks. Plot is based on data from Figure 4 of Baum, Reinhart, and Ferguson (1998). SAA contours M2, M25 and M27 are marked.

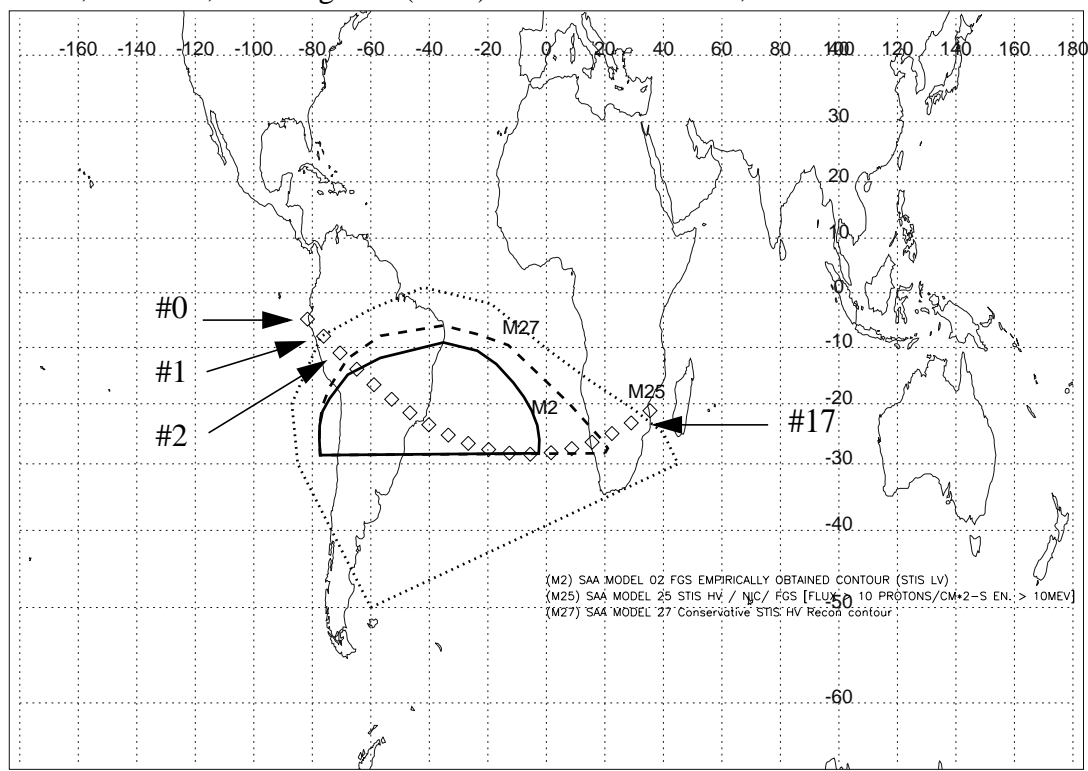
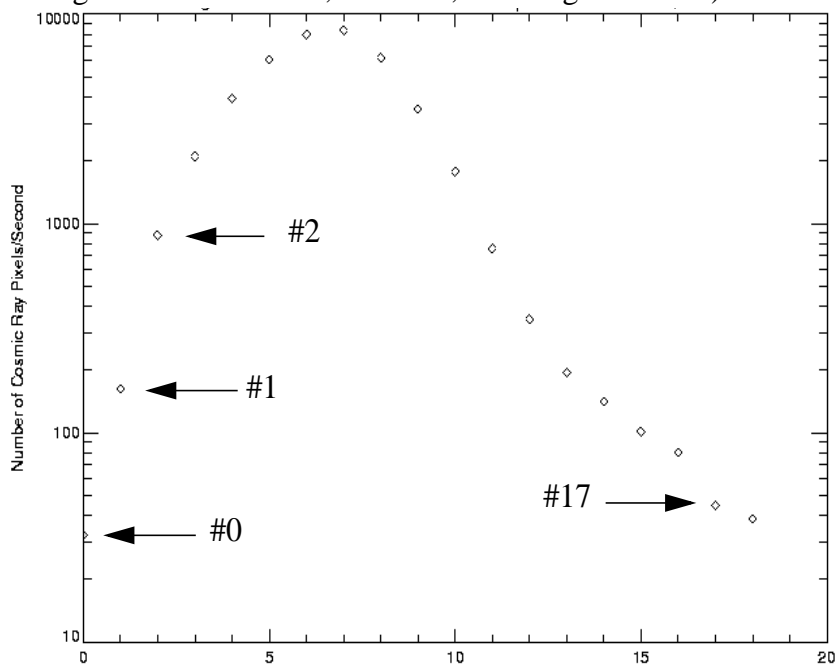


Figure 6: Cosmic ray rates for the STIS CCD 60s darks in Figure 5, in units of pixels / sec (reproduction of Figure 3b from Baum, Reinhart, and Ferguson 1998).



Again these data show a similar effect -- rates are low just inside the M25 contour on the east side of the SAA, but are quite high just inside M25 on the west side of the SAA. For example, point #17 (lat -25, long +28), just inside the east end of the M25 contour, has a rate of ~40 pixels / sec. On the west side, the rate at point #1 (lat -8, long -78), just at the M25 contour, is ~170 pixels / sec, while the rate at point #2 (lat -11, long -70), just inside the contour, is ~900 pixels / sec. The rate of STIS cosmic rays for data taken away from the SAA is about 28 pixels / sec. That is, the rates on the east side are within a factor of two of “nominal,” while on the west side, the rates quickly rise to 30 or more times nominal.

We note that the STIS rates appear higher than the WFPC2 rates (Figure 1c), primarily because we have only counted pixels above 20 DN as cosmic rays whereas the STIS analysis included all pixels with elevated counts in each cosmic ray “hit.” Differences in detector area and pixel size will also contribute to the differences in the measured cosmic ray rates between STIS and WFPC2.

5. Discussion and Revisions to the WFPC2 SAA Avoidance Contour

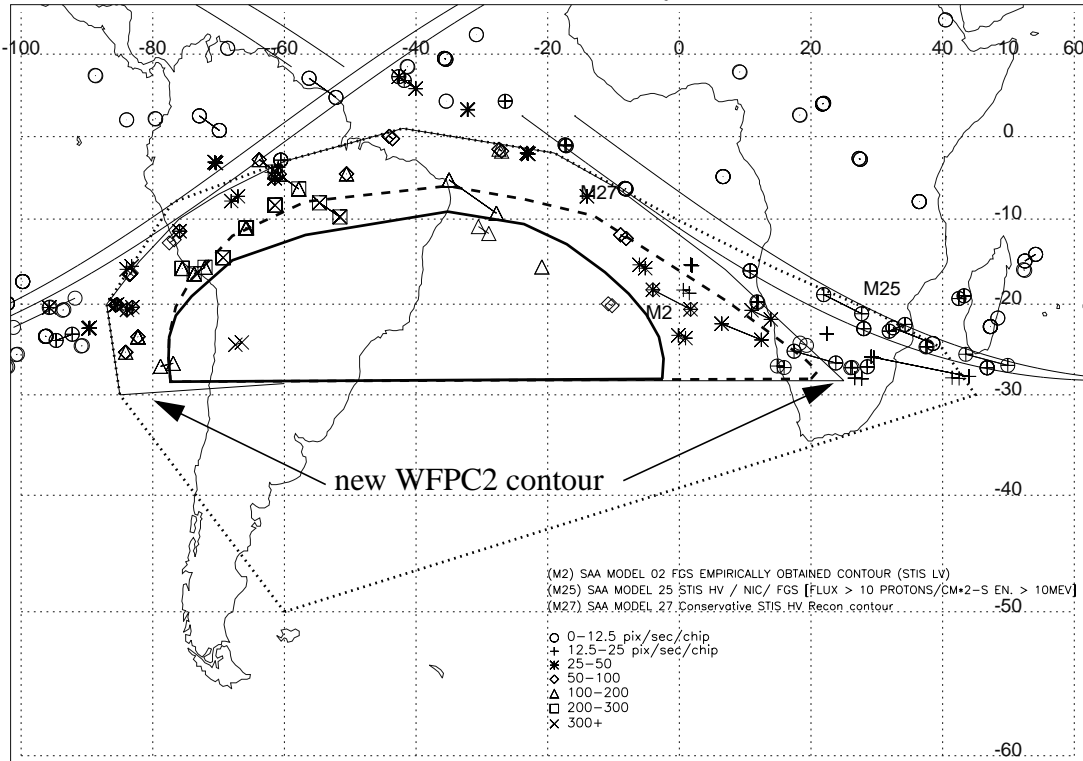
The proposed revision to the WFPC2 SAA avoidance contour is illustrated in Figure 6. On the east side of the SAA, the new contour lies just outside the M27 (STIS) contour; on the north and west sides of the SAA, the new contour is nearly identical to the old M25 (WFPC2) contour. We have made one small change on the northwest side of the SAA, smoothing out a vertex of the M25 contour. This corner was reducing the number of SAA-free orbits yet appeared to be artificial in nature (i.e. it did not correspond to any structure in the observed cosmic ray distribution).

The new WFPC2 contour increases the available SAA-free orbital longitude by ~12 degrees. Given that the Earth rotates ~22 degrees per HST orbit, this corresponds to an additional ~0.55 SAA-free orbits per day on average.

The risks posed to WFPC2 images by the new contour are relatively modest. Essentially all the change occurs on the east side of the SAA. The worst-case scenario occurs for orbits where HST is moving tangentially to the SAA contour on the east side of the orbit. For these orbits, it is possible for an entire 600 sec exposure to be executed inside the old M25 contour, resulting in exposure to cosmic ray rates of 2 to 4 times the mean orbital value. Such images would be seriously affected, but fortunately, are also quite rare. The new contour occupies about 8 degrees of orbital longitude on the east side of the SAA, only about one-tenth the duration of an orbit. Thus, it affects only about 0.2% of the orbital area. In addition, it is unlikely that an exposure would start exactly as HST enters the region inside the new contour. And, many exposures are either much longer or shorter than 600 sec: longer images see less fractional increase in cosmic rays, while images $\ll 600$ sec see fewer total cosmic rays. Hence, we estimate the fraction of WFPC2 images seriously affected by the new contour to be $<0.1\%$, or <6 science images per year.

For orbits where HST passes directly through the SAA (as opposed to moving tangentially to the SAA contour), there is very little impact. In these cases, the time HST spends between the new and old contours would usually be occupied with target acquisition activities, rather than imaging.

Figure 7: Distribution of cosmic ray rate around the SAA with the revised WFPC2 SAA avoidance contour indicated (thin solid line). Curved lines indicate the HST orbit at points where it runs tangent to the old WFPC2 contour (M25, dotted line) and the new contour.



6. Acknowledgements

We thank PRESTO, SESD, and SSD personnel for technical support and useful discussions during this investigation, including Vicki Balzano, John Baum, Stefi Baum, Stefano Casertano, George Chapman, David Elkin, Matt Lallo, Olivia Lupie, Chris Odea, Merle Reinhart, Bill Sawchuck, Peggy Stanley, and Brad Whitmore.

7. References

- Baum, S., Reinhart, M., and Ferguson, H. 1998, STIS TIR 98-10.
Lindler, D., 1997, memo "STIS CCD Cosmic Ray Hits vs. Orbital Position"
Reinhart, M., 1998, private communication.